RSC Advances

PAPER

View Article Online
View Journal | View Issue

Check for updates

Cite this: *RSC Adv.*, 2019, **9**, 34330

Effects of octamethylcyclotetrasiloxane grafting and *in situ* silica particle generation on the curing and mechanical properties of a styrene butadiene rubber composite

Changjie Yin * and Qiuyu Zhang

Received 17th July 2019
Accepted 11th October 2019

DOI: 10.1039/c9ra05475h

rsc.li/rsc-advances

The reinforcement of octamethylcyclotetrasiloxane (D_4) grafted styrene butadiene rubber (SBR-*g*-D_4) with *in situ* generated silica was performed using the sol–gel reaction of tetraethoxysilane (TEOS) in latex. The characterization of SBR-*g*-D_4 and *in situ* generated silica reinforced SBR-*g*-D_4 was investigated by Fourier transform infrared spectroscopy (FTIR), X-ray photoelectron spectroscopy (XPS) and Raman spectroscopy. The grafting efficiency of the styrene butadiene rubber (SBR) was determined by a gravimetric method. It was found that the constant silicon content and the grafting efficiency of SBR were 1.72% and 0.13 wt% when the weight ratio of D_4 to SBR was 0.20. The effects of the D_4 and *in situ* generated silica content on the curing characteristics, mechanical properties and morphology of SBR latex were investigated. The mechanical properties of *in situ* generated silica reinforced SBR-*g*-D_4 vulcanizates were improved significantly compared to raw SBR vulcanizate when the *in situ* generated silica content was 18.05%. Compared with silica reinforced SBR-*g*-D_4, the tensile strength, wet skid resistance and rolling resistance of the *in situ* generated silica reinforced SBR-*g*-D_4 were better. This is because of the higher crosslinking degree in the SBR-*g*-D_4 matrix and the strong chemical bond between SBR-*g*-D_4 molecular chains and *in situ* generated silica. Scanning electron microscopy analysis revealed good silica filler dispersion in all the reinforced SBR-*g*-D_4 vulcanizates.

1. Introduction

As previously reported,[1–3] silica (SiO_2) is considered to be a good candidate for the substitution of the traditional carbon black in the application of green tire manufacturing, because the tire treads filled by silica have better wet skid resistance, low rolling resistance and better wear resistance than carbon.[4,5] However, SiO_2 has a high polarity and hydrophilic surface due to silanol groups on its surface,[6] which leads to poor interactions between SiO_2 and SBR.[7]

In order to solve this problem, the grafting modification of SBR is a promising and effective approach.[8] In previous work, many studies focused on grafting rubber using the vinyl monomers, such as maleic anhydride (MA),[9] vinyl alcohol (VA),[10] stearyl methacrylate,[11] methyl methacrylate (MMA),[12] glycidyl methacrylate (GMA),[13] acrylonitrile (AN),[14] styrene (St),[15] vinyltriethoxysilane[16] and so forth. The methods for the preparation of grafted rubber include thermal graft copolymerization[17–20] and irradiation grafting polymerization.[21–23] Second, the generation of the *in situ* silica in the rubber matrix by the sol–gel reaction of TEOS is another effective technology, and this technology has been used in various rubber forms, such as solid rubber,[24,25] rubber latex[26,27] and rubber solution.[28–30] Third, combining the grafted rubber with sol–gel technology using TEOS to improve the properties of silica/rubber compounds is the most effective method of all. Sittiphan *et al.*[31] reported the filling of styrene (St) grafted natural rubber (St-NR) with *in situ* generated silica which was performed using the sol–gel reaction of TEOS, where transmission electron microscopy results revealed that the *in situ* silica particles were small (~40 nm in diameter) and well dispersed. The *in situ* silica filling of MMA-NR *via* the solid rubber and rubber latex methods has been reported.[32] Although the use of vinyl monomer graft polymerization modified rubber can improve the compatibility between silica and rubber, the chemical interaction between rubber and SiO_2 has not been greatly improved. Zhang *et al.*[33,34] discussed the *in situ* silica reinforcement of VTES grafted SBR (SBR-*g*-VTES) by the sol–gel process in latex; it was reported that the increased tensile strength was due to the chemical interaction between silica and SBR in the *in situ* reinforced SBR-*g*-VTES. However, with the grafting polymerization of the VTES onto the SBR in latex, the hydrolysis and condensation of the VTES may destroy the stability of SBR latex. Therefore, it is highly necessary to use unhydrolyzable cyclosiloxanes to obtain the grafted

---

Xi'an Key Laboratory of Functional Organic Porous Materials, Department of Applied Chemistry, School of Science, Northwestern Polytechnical University, Xi'an, Shaanxi 710072, People's Republic of China. E-mail: yinchangjie@nwpu.edu.cn

SBR. Recently, different methods of grafting octamethylcyclotetrasiloxane (D_4) onto polyacrylate by emulsion polymerization have been reported. Liang *et al.*[35] prepared a new core–shell silicon-containing fluoroacrylate by the D_4 ring-opening polymerization in the presence of the fluoroacrylate latex using ammonium persulfate (APS) as the initiator. Jiang *et al.*[36] also thoroughly studied the kinetics of the ring-opening polymerization of D_4 in emulsion, showing that the content of D_4 molecules at the interface could cause an increase in the polymerization rate. Based on these two articles, it is possible to obtain modified polymers by ring-opening polymerization of D_4 in emulsion.

As a result, in this study, the SBR-*g*-D_4 (D_4 grafted SBR) was firstly synthesized using the grafting polymerization reaction of the D_4 onto the SBR molecular chains in the SBR latex. The effects of the D_4 content on the silica content, curing characteristics and mechanical properties of the SBR-*g*-D_4 were investigated to find the optimal conditions (defined as a good balance between curing characteristics and mechanical properties at the highest grafting ratio of SBR with the lowest added mass of D_4). The SBR-*g*-D_4 latex was then mixed with various amounts of TEOS at 50 °C. Subsequently, SBR composites with a different silica content were obtained after the *in situ* sol–gel of TEOS. The effects of the mass of TEOS on the silica content, utilization of the TEOS, curing characteristics and mechanical properties of *in situ* generated silica reinforced SBR-*g*-D_4 vulcanizates were systematically discussed. Finally, the morphology of the *in situ* silica filled SBR-*g*-D_4 vulcanizates was characterized.

The schematic representation of the *in situ* silica generated in the SBR-*g*-D_4 matrix after graft copolymerization is shown in Scheme 1. The occurrence of the D_4 grafting onto the SBR backbone (Scheme 1a) and the formation of the *in situ* silica *via* the sol–gel reaction of TEOS in the TEOS swelled SBR-*g*-D_4 latex, for sol–gel reaction after graft copolymerization, are depicted. The chemical bond could be formed between the *in situ* generated silica particles and SBR-*g*-D_4 molecular chains (Scheme 1b).

2. Experimental

2.1 Materials

Silica was purchased from Changtai Micro-Nano Chemistry Co., Ltd., China. The primary silica particles were of 10–20 nm diameter and with a 190 $m^2\ g^{-1}$ to 200 $m^2\ g^{-1}$ surface area. The styrene butadiene rubber (SBR1502) was kindly provided by Lan Zhou Petroleum Chemical Industrial Co., Ltd., China. Octamethylcyclotetrasiloxane (D_4) was provided by Guangzhou Double Peach Fine Chemical Co., Ltd., China. Tetraethoxysilane (TEOS, CP) was purchased from Sinopharm Chemical Reagent Co., Ltd., China. Potassium persulfate (KPS, CP) was supplied by Tianjin Shan Pu Chemical Co., Ltd., China. Sulfur, zinc oxide (ZnO), stearic acid (SA), *N*-cyclohexyl-benzothiazyl-sulfenamide (CBS, purity > 97%), *N*-(1,3-dimethylbutyl)-*N*′-phenyl-*p*-phenylenediamine (DPG, purity > 97%), 2,2,4-trimethyl-1,2-dihydroquinoline (8PPD), methyltrialkylammonium chloride (AM-2) and the condensation product of dicyandiamide and formaldehyde (TXD), both industry grade, were provided by Lan Zhou Petroleum Chemical Industrial Co., Ltd., China.

2.2 Preparation of D_4 grafted SBR (SBR-*g*-D_4)

The graft reactions were carried out in a four neck 500 mL round bottom flask reactor with agitation of 100 rpm under nitrogen atmosphere. In each reaction, 200.00 g SBR latex (40.00 g dry SBR) was added first while stirring at 80 °C over 30 min to remove the oxygen. The initiator KPS (1.00 g KPS was dissolved in 9.00 g H_2O) was then added in turn to the latex over 60 min, while at the same time, the D_4 (varying from 0.00 g, 2.00 g, 4.00 g, 6.00 g, 8.00 g, 10.00 g) was slowly dropped into the latex at a rate of 20 mg min^{-1} until completion; stirring was continued for 1 hour to obtain the grafted SBR latex (SBR-*g*-D_4 latex). Hydroquinone was added to stop the reaction. 24 hours later 2.00 g SBR-*g*-D_4 latex samples were poured on a vessel and dried in an oven at 70 °C for 48 h to remove water and unreacted monomers to obtain the dry SBR-*g*-D_4 which was used for infrared and thermogravimetric analysis.

2.3 Sol–gel reaction of TEOS in the SBR-*g*-D_4 latex

In this study, the TEOS was added after the graft copolymerization. The TEOS was slowly dropped into the SBR-*g*-D_4 latex at a rate of 0.50 g min^{-1} at 50 °C until completion; the conditions for the sol–gel reaction of TEOS in SBR-*g*-D_4 latex are summarized in Table 1. The antioxidant (0.010 g 8PPD) and coagulants (0.020 g AM-2, and 0.001 g TXD) were then added into the *in situ* sol–gel SBR-*g*-D_4 latex by dropping in turn over 2 min, and then the SBR-*g*-D_4 rubber was coagulated from the latex. Lastly, the SBR-*g*-D_4 rubber was dried under vacuum at 60 °C for 24 h.

2.4 Preparation of silica reinforced SBR vulcanizates and the *in situ* generated silica reinforced SBR-*g*-D_4 vulcanizates

The compounding compositions of the silica and *in situ* generated silica reinforced SBR-*g*-D_4 vulcanizates are described in Table 2. The *in situ* generated silica reinforced SBR-*g*-D_4 vulcanizates were obtained using a two-roll mill (X(S)-160 type at room temperature, Shanghai Rubber Machinery Factory, China). First, the *in situ* formed silica reinforced SBR-*g*-D_4 rubber, ZnO and SA were mixed together by a two-roll mill. Second, the S, and the vulcanization accelerators CBS and DPG, were added into the same mill. Third, the rubber composites were vulcanized at 160 °C according to the optimum cure time (t_{90}) measured by a rubber rheometer in a press at 10 MPa to obtain the 2.00 mm thick films of vulcanized rubber to be used in the mechanical properties analysis.

2.5 Characterization

2.5.1 Silicon content and grafting efficiency of SBR. Ungrafted SBR was washed out in a Soxhlet extractor with 60–80 °C boiling point petroleum ether for 24 h, and the residue was then extracted in acetone for 24 h to remove the free polymers of D_4. The grafting efficiency of D_4 (w) = practical silicon content (w_2)/theoretical silicon content (w_1). The formulae for calculating w_1 and w_2 are as follows:

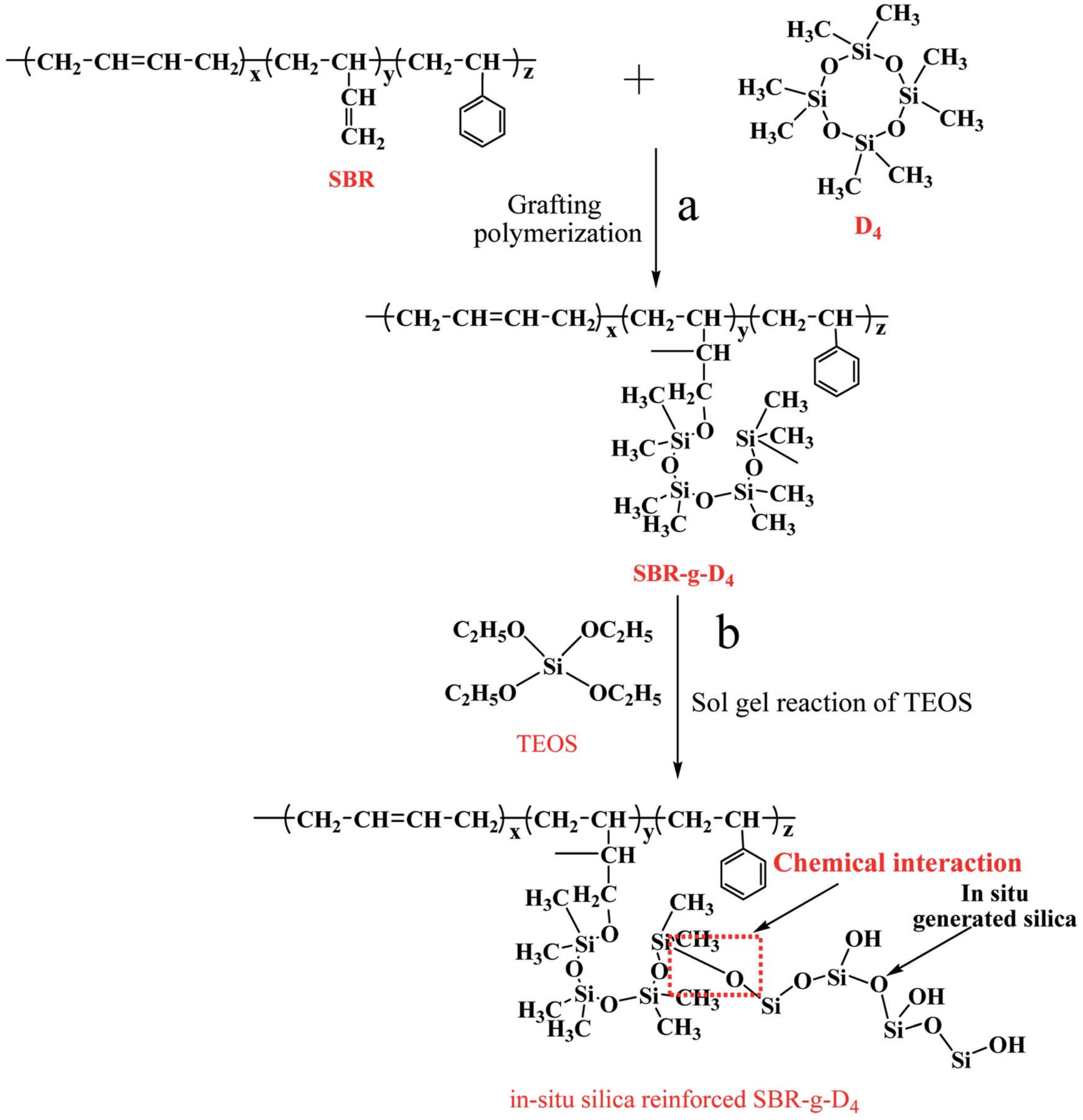

Scheme 1 Possible mechanism for the interactions and bonding between SBR-*g*-D_4 and silica.

$$w_1 = \frac{m_2 \times 4 \times 28}{296 \times m_1} \tag{1}$$

$$w_2 = \frac{m_4 \times 28}{m_3 \times 60} \tag{2}$$

$$w_0 = \frac{m_2 \times w}{m_2 \times w + 40.00} \tag{3}$$

w_0 represents the grafting efficiency of SBR; m_1, m_2 represent the total mass of the SBR-*g*-D_4 and D_4, respectively; m_3 denotes the weight of SBR-*g*-D_4 for muffle furnace burning; m_4 denotes the weight of the ashes (the residue of SBR-*g*-D_4 in a muffle furnace under 700 °C for 6 h, washed by diluted hydrochloric acid and water three times, respectively). 4, 40, 28, 60 and 296 are the number of silicon atoms in D_4, the quality of dry rubber, the molecular weight of silicon, silica and D_4, respectively.

2.5.2 Silica content and utilization of silica in the *in situ* formed silica reinforced SBR-*g*-D_4.

The silica content and utilization efficiency of TEOS were determined using a muffle furnace under 700 °C for 6 h. Silica content (w_3) = m_6/m_5, utilization efficiency of TEOS = practical silica content as

Table 1 Conditions for the sol–gel reaction of TEOS in the SBR-*g*-D_4 latex

Condition number	TEOS content (g)	Temperature (°C)
1	0.00	50
2	2.00	50
3	4.00	50
4	6.00	50
5	8.00	50
6	10.00	50

Table 2 Formulations for the rubber compounding, in parts by weight per hundred parts (phr)

Ingredient	Content (phr)	Content (phr)	Content (phr)
Pristine SBR	100.00		
SBR-*g*-D_4 rubber		100.00	
In situ reinforced SBR-*g*-D_4 rubber			100.00
Silica	0	Varied from 0, 4.80, 7.90, 9.32, 13.70, 18.05	0
ZnO	3.00	3.00	3.00
SA	1.00	1.00	1.00
CBS	1.00	1.00	1.00
DPG	1.50	1.50	1.50
S	2.00	2.00	2.00

formed by TEOS (w_5)/theoretical silica content as formed by TEOS (w_4). The formulae for calculating w_4, w_5, and w_6 are as follows:

$$w_4 = \frac{m_7 \times 60/208}{200 \times 20\% + m_7 \times 60/208} \tag{4}$$

$$w_6 = \frac{m_8 \times 60/297}{200 \times 20\% + m_8 \times 60/297} \tag{5}$$

$$w_5 = w_3 - w_6 \times w \tag{6}$$

where m_5, m_6 are the weight of *in situ* generated silica reinforced SBR-*g*-D_4 and the weight of the residue of *in situ* generated silica reinforced SBR-*g*-D_4 in a muffle furnace under 700 °C for 6 h, respectively. m_7 and m_8 are the weight of TEOS and D_4, respectively. 60, 297, 208, and w are the molecular weights of SiO_2, D_4, TEOS, and the grafting efficiency of D_4, respectively. Bound rubber was measured as a percentage of insoluble rubber in total rubber for the differing silica content.

2.5.3 ATR-FTIR analysis. The attenuated total reflectance-Fourier transform infrared (ATR-FTIR) spectra of SBR, SBR-*g*-D_4 and *in situ* generated silica reinforced SBR-*g*-D_4 were characterized using a Tensor-37 FTIR spectrometer (Bruker Optics Inc, Germany) at room temperature. The FTIR spectrum of D_4 was determined in the range of 400–4000 cm^{-1} with 32 scans.

2.5.4 XPS analysis. The XPS analysis of SBR and SBR-*g*-D_4 rubber samples was conducted using a Kratos Axis Ultra X-ray photoelectron spectrometer fitted with a monochromatic Al Kα X-ray source (1487 eV) operating on a spot size of 300 μm.[37]

2.5.5 Raman spectroscopy. The Raman spectra of SBR and SBR-*g*-D_4 were recorded using a WITec alpha 300RA confocal Raman spectrometer.[38]

2.5.6 Curing characteristics. The curing time (t_{90}), maximum torque (MH) and minimum torque (ML) of rubber vulcanizate composites were studied using a Moving Die Rheometer (MDR) JC-2000E (JiangDu JingCheng Test Instruments Factory, China) at 160 °C according to ASTM D 2084-95.

2.5.7 Mechanical properties. The mechanical properties of the 2 mm thick cured films of the rubber vulcanizate composites were measured using a SANS-CMT 5105 electrical tensile tester (Shenzhen SANS Test Machine Co., China) in accordance with ASTM D 412 using dumbbell-shaped test specimens at a crosshead speed of 500 mm min^{-1}.

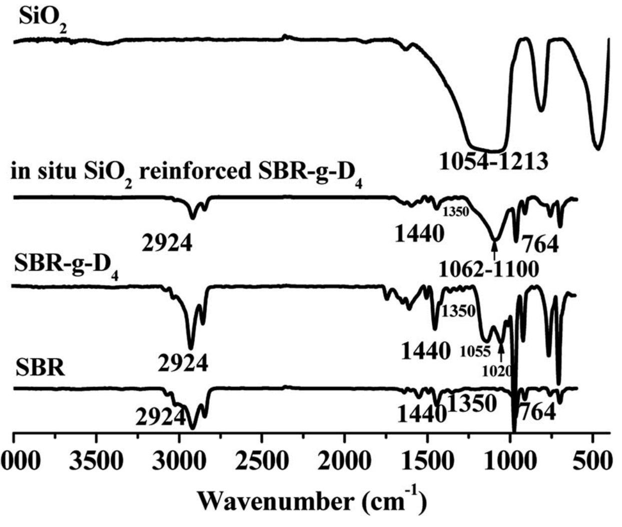

Fig. 1 FTIR spectra of SBR, SBR-*g*-D_4, *in situ* generated SiO_2 reinforced SBR-*g*-D_4 and SiO_2.

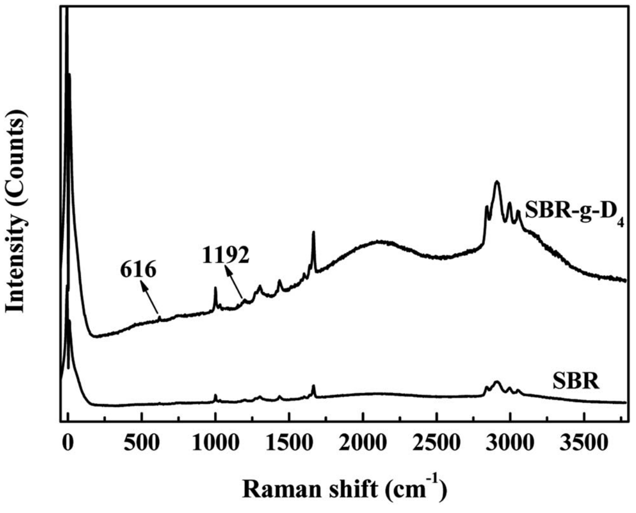

Fig. 2 Raman spectra of SBR and SBR-*g*-D_4.

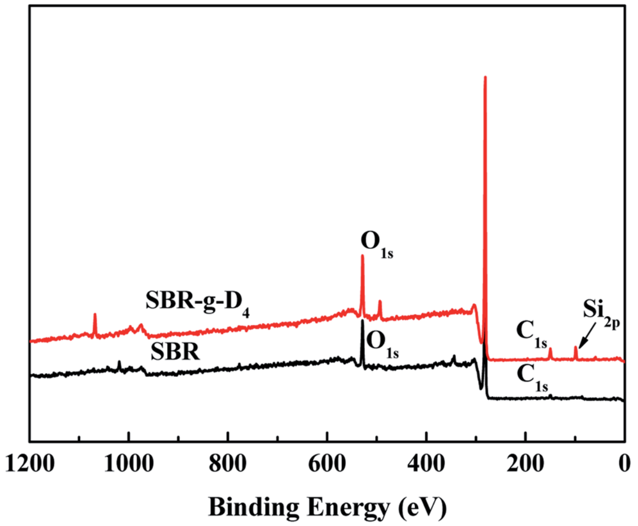

Fig. 3 XPS spectra of SBR and SBR-*g*-D_4.

2.5.8 Dynamic mechanical analysis. Dynamic mechanical analysis was performed using the DMA/SDTA861e (Mettler-Toledo, Switzerland) in the tension mode, at a heating rate of 5°C min^{-1} from −50 °C to 110 °C. The specimens (size 30 × 5 × 2 mm^3) were cut from the center of the samples.

2.5.9 Scanning electron microscopy (SEM). Examination of the tensile fracture surfaces of SBR and the *in situ* formed silica reinforced SBR-*g*-D_4 composites was conducted using SEM with a JSM-6700F scanning electron microscope (Japan Electron Optics Laboratory, Japan) on gold-coated cryo-fracture surfaces.

3. Results and discussion

3.1 Characterization of SBR-*g*-D_4 and *in situ* generated SiO_2 reinforced SBR-*g*-D_4

FTIR spectra of the pristine SBR, pristine silica, SBR-*g*-D_4, and *in situ* generated silica reinforced SBR-*g*-D_4 without any cross-linking additives are shown in Fig. 1. For SBR, the absorption peaks appeared at 2924, 1440, 1350 and 764 cm^{-1}, which were identified as the stretching vibration of aliphatic =C–H, C–H bending of CH_2, C–H bending of CH_3 and C=C bending vibrations, respectively.[32]

Compared with the pristine SBR, the spectrum of the SBR-*g*-D_4 shows the same major signals as obtained from SBR, and the additional absorption signals at 1020 and 1055 cm^{-1} corresponding to the –Si–O–C– and –Si–O–Si–[39] stretching and vibration are evidence for D_4 being present in the SBR-*g*-D_4 grafted copolymer.

Furthermore, the new absorption peaks at 1062–1100 cm^{-1} are attributed to the –Si–O–Si– stretching of silica generated by the sol–gel reaction of the TEOS in the *in situ* generated SiO_2 reinforced SBR-*g*-D_4.[40] Compared with the absorption peaks of –Si–O–Si– groups at 1054–1213 cm^{-1} in the pristine silica, the narrower absorption peaks in the SiO_2 reinforced SBR-*g*-D_4 may indicate the existence of an interaction between SBR-*g*-D_4 and silica that arises *via* D_4.

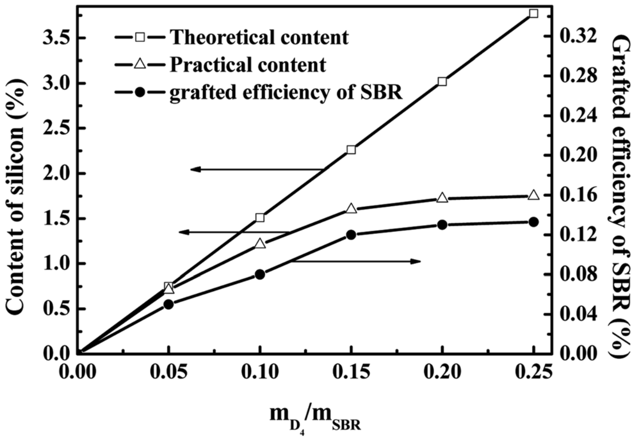

Fig. 4 Effects of the weight ratio of D_4 to SBR on the silicon content in SBR-*g*-D_4.

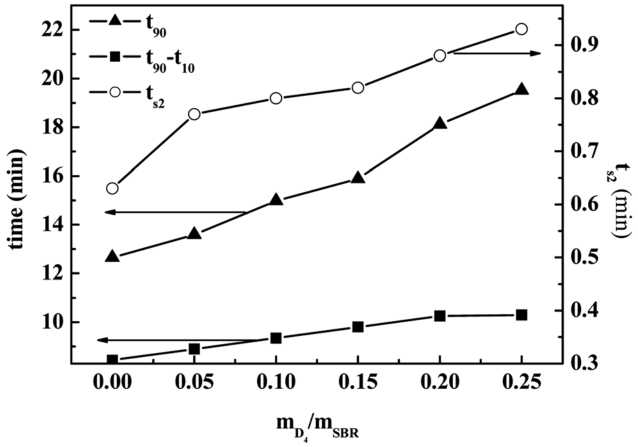

Fig. 5 Effects of the weight ratio of D_4 to SBR on the cure time (t_{90}) and scorch time (t_{s2}) of the SBR-*g*-D_4 vulcanizates.

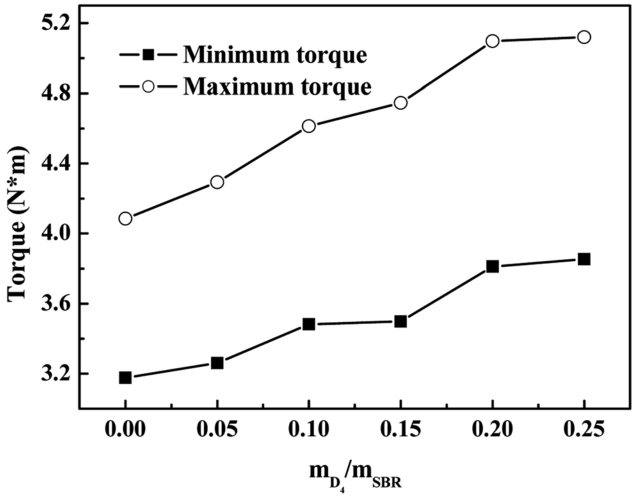

Fig. 6 Effects of the weight ratio of D_4 to SBR on the maximum torque (MH) and minimum torque (ML) of the SBR-*g*-D_4 vulcanizates.

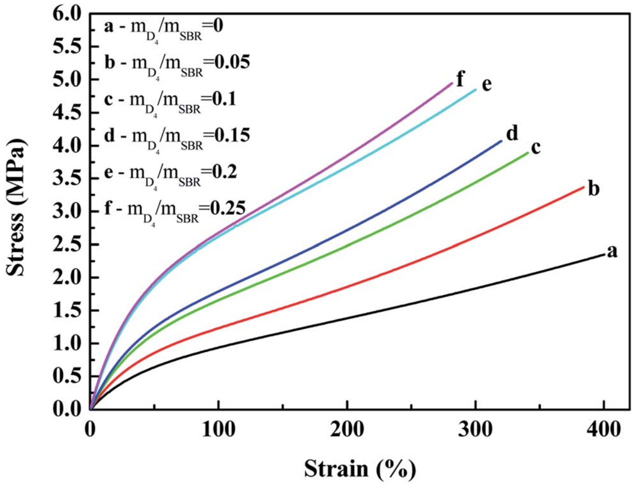

Fig. 7 Effects of the weight ratio of D_4 to SBR on the stress–strain behavior of the SBR-*g*-D_4 vulcanizates.

Raman spectra were obtained to confirm that the D_4 was grafted onto the backbone of SBR. The corresponding results are shown in Fig. 2. Compared with the Raman spectrum of SBR, the new peaks at 616 and 1192 cm^{-1} could be assigned to the bending and asymmetric stretching modes in the Si–O–Si for D_4, respectively.[41] At the same time, the non-polar $-CH_3$ groups are at the Raman shift of 2900–3000 cm^{-1}, and it is shown that the band peak at 2900–3100 cm^{-1} for the SBR-*g*-D_4 is much stronger than that of SBR, which indicates that a large number of $-CH_3$ groups have been introduced into the molecular chains of the SBR after grafting with D_4.

The elemental composition of SBR and SBR-*g*-D_4 samples was analyzed with wide-scan XPS spectra, as shown in Fig. 3. Compared with SBR alone, for the SBR-*g*-D_4 sample, stronger O_{1s} and C_{1s} signals were observed, and a new peak at 98–100 eV corresponding to Si element was also observed for the SBR-*g*-D_4 sample, indicating the successful grafting of D_4 onto SBR chains.[42]

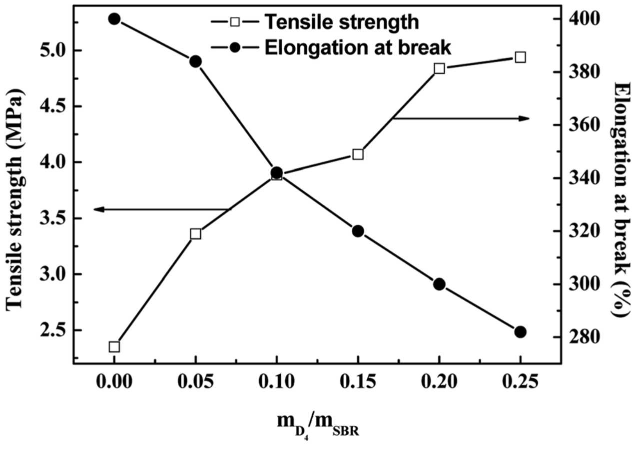

Fig. 8 Effects of the weight ratio of D_4 to SBR on the tensile strength and elongation at break of the SBR-*g*-D_4 vulcanizates.

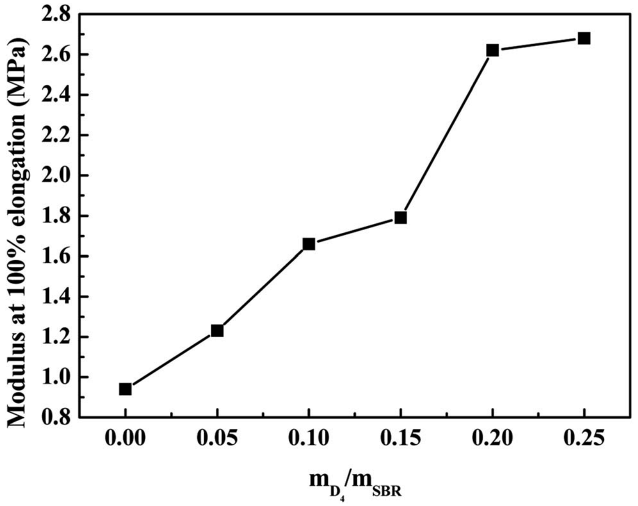

Fig. 9 Effects of the weight ratio of D_4 to SBR on the modulus at 100% elongation of the SBR-*g*-D_4 vulcanizates.

In this experiment, octamethylcyclotetrasiloxane (D_4) was chosen to be grafted onto the molecular chains of SBR. From the results of the FTIR, Raman and XPS analysis, the main reaction is the free radical polymerization between the ring-opening of D_4 with the double bond in SBR as in Scheme 1. The ring-opening polymerization of D_4 was initiated by KPS to get the active center in the SBR latex, and then one part of the active center could attack the double bond in the molecular chains of SBR to obtain the SBR-*g*-D_4, and one part of the active center could form ungrafted polyoctamethylcyclotetrasiloxane. Huang *et al.* also found that polyacrylate modified by polysiloxane latex could be successfully prepared by successive seeding polymerization with the radical polymerization of acrylate and the ring opening polycondensation of D_4.[43]

3.2 Graft copolymerization of D_4 onto SBR latex

3.2.1 Silicon content in the SBR-*g*-D_4 and grafting efficiency of SBR. The effects of the weight ratio of D_4 to SBR on the

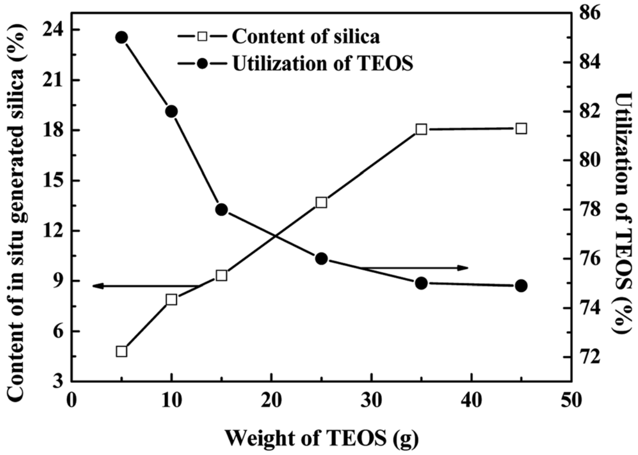

Fig. 10 Effects of the weight of TEOS on the *in situ* generated silica content and utilization of TEOS.

Table 3 Effects of *in situ* generated silica content on the curing time of reinforced SBR-*g*-D_4 vulcanizates

In situ generated silica (%)	t_{s2} (min)	t_{90} (min)	t_{90}–t_{10} (min)
0	0.82	15.89	8.50
4.8	1.13	16.41	8.98
7.9	1.23	17.63	9.21
9.32	1.32	18.75	9.35
13.7	1.56	19.34	9.48
18.05	1.73	20.5	9.62

practical silicon content, theoretical silicon content and grafting efficiency of SBR were studied and are shown in Fig. 4. This shows that the practical silicon content was lower than the theoretical silicon content in the SBR-*g*-D_4; this is due to the free PD_4 (polyoctamethylcyclotetrasiloxane) which is increased with increasing the mass ratio of D_4 to SBR, with similar results having been observed by Satraphan *et al.*[44] and Kochthongrasamee *et al.*,[45] who suggested that the homopolymerization was more pronounced than the graft copolymerization at higher monomer concentrations, and thus, the free PD_4 increased and the silicon content in the SBR-*g*-D_4 decreased.

For the practical silicon content (PCS) and grafting efficiency of SBR (GER), these increased with increasing the weight ratio of D_4 to SBR; however, they remained constant when the weight ratio of D_4 to SBR was higher than 0.20, as shown in Fig. 4. The constant silicon content and GER were 1.72% and 0.13 wt% when the weight ratio of D_4 to SBR was 0.20. This is due to the fact that the inter-molecule crosslinking reactions of SBR probably occurred throughout the grafting polymerization,[10] and the formed cross linking network structure could prevent the free D_4 monomers from reacting with the SBR molecular chains, resulting in the constant GER at the higher weight ratio of D_4 to SBR.

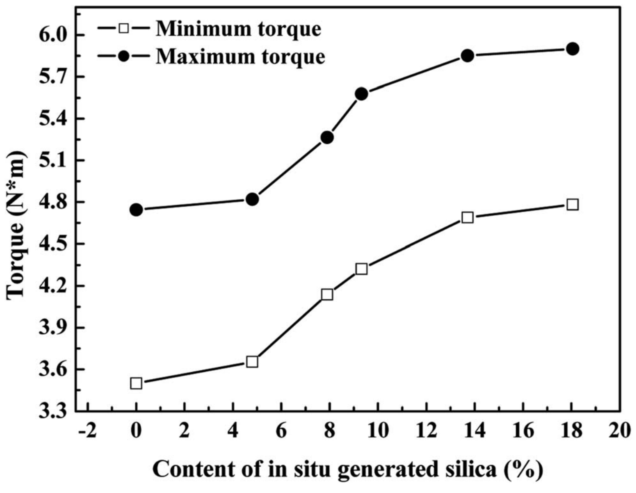

Fig. 11 Effects of *in situ* generated silica content on the torque of reinforced SBR-*g*-D_4 vulcanizates.

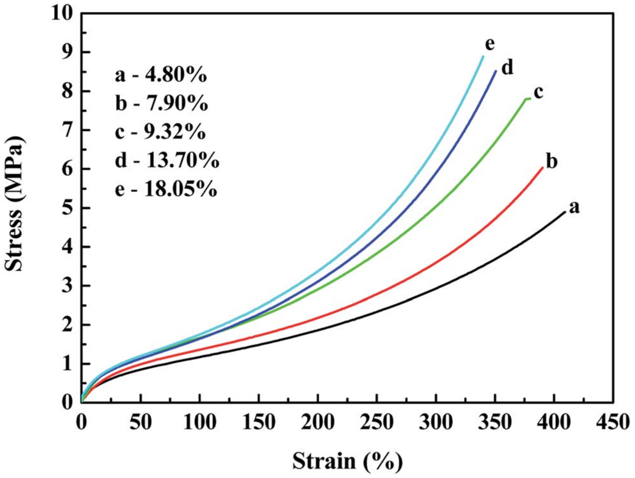

Fig. 12 Effects of the silica content on the stress–strain behavior of silica reinforced SBR-*g*-D_4.

3.2.2 Curing characteristics of SBR-*g*-D_4 vulcanizates. Scorch time (t_{s2}) and optimum cure time (t_{90}) of the SBR-*g*-D_4 vulcanizates are shown in Fig. 5 t_{s2} is a measure of the time to premature vulcanization while t_{90} is the optimum cure time of the vulcanizates. It can be seen that both the t_{s2} and t_{90} of the vulcanizates were prolonged with increasing the weight ratio of D_4 to SBR. This might be due to the high polarities of –Si–O–Si– groups which interfere with the vulcanization, that is, some of the –Si–O–Si– groups in the D_4 are assumed to have interacted with –C=C– groups in the molecular chains of SBR; the remaining free –Si–O–Si groups could possibly form hydrogen bonds with polar accelerators, causing accelerator adsorption on the polar surface.[46]

The value of t_{90}–t_{10} can represent the increasing speed of the degree of rubber crosslinking. As also shown in Fig. 5, the value of t_{90}–t_{10} increased significantly with increasing the weight ratio of D_4 to SBR, and this remained constant when

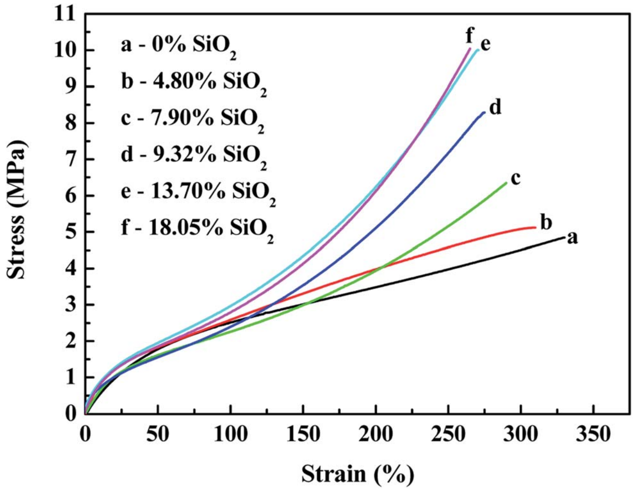

Fig. 13 Effects of the silica content on the stress–strain behavior of *in situ* generated silica reinforced SBR-*g*-D_4.

Table 4 Effects of the silica content on the tensile strength and elongation at break of the silica reinforced SBR-*g*-D_4 and *in situ* generated silica reinforced SBR-*g*-D_4 vulcanizates

Silica content (%)	*In situ* generated silica reinforced SBR-*g*-D_4		Silica reinforced SBR-*g*-D_4	
	Tensile strength (MPa)	Elongation at break (%)	Tensile strength (MPa)	Elongation at break (%)
4.80	5.12 ± 0.03	309.99 ± 5.11	4.89 ± 0.02	409.20 ± 5.39
7.90	6.35 ± 0.02	289.56 ± 6.23	6.03 ± 0.03	390.24 ± 7.10
9.32	8.29 ± 0.02	275.00 ± 3.09	7.81 ± 0.02	379.58 ± 2.95
13.70	10.00 ± 0.01	270.79 ± 3.55	8.52 ± 0.03	350.68 ± 4.02
18.05	10.04 ± 0.04	265.01 ± 2.89	8.89 ± 0.04	340.01 ± 6.03

the weight ratio of D_4 to SBR was higher than 0.20. Compared with the crosslinking degree of pristine SBR, the crosslinking degree of SBR-*g*-D_4 containing the additional –Si–O–Si– linkage crosslinking caused by the ring-opening polymerization in the SBR-*g*-D_4 (ref. 47) is enhanced, and thus, the greater the SBR-*g*-D_4 content, the faster the increasing speed of the degree of rubber crosslinking. Meanwhile, the SBR-*g*-D_4 content is determined by the GER which is shown in Fig. 4; as a result, the changes in t_{90}–t_{10} are consistent with the GER data.

Fig. 6 shows the effects of the weight ratio of D_4 to SBR on the maximum torque (MH) and minimum torque (ML) of the SBR-*g*-D_4; it shows that the MH and ML increased with increasing the weight ratio of D_4 to SBR. The small number of grafted D_4 chains could enhance interaction between SBR molecular chains, causing the increased MH and ML.

3.2.3 Mechanical properties of SBR-*g*-D_4 vulcanizates. Fig. 7 shows the effects of the weight ratio of D_4 to SBR on the stress–strain behavior of the SBR-*g*-D_4 vulcanizates. It can be seen that the high D_4 content in the SBR-*g*-D_4 is beneficial in improving the modulus of the SBR-*g*-D_4 vulcanizates, which reflects an increase in the cross-linking density of SBR-*g*-D_4 chains.[48]

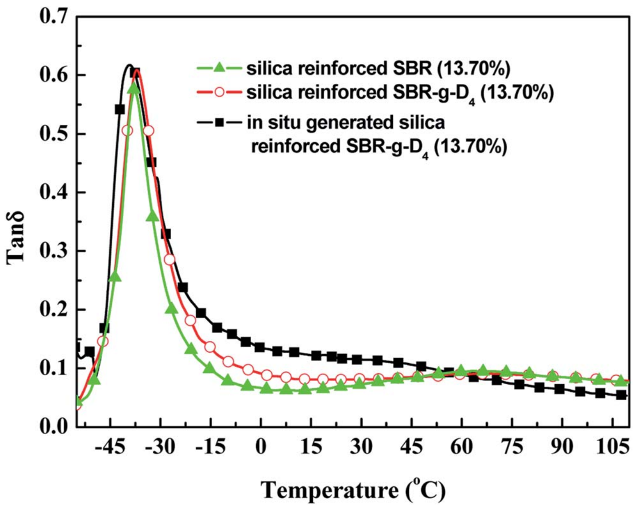

Fig. 14 Temperature dependence of tan δ (−50 to 110 °C) for silica reinforced SBR, SBR-*g*-D_4 and *in situ* generated silica reinforced SBR-*g*-D_4.

The effects of the weight ratio of D_4 to SBR on the tensile strength, elongation at break and the modulus at 100% elongation are presented in Fig. 8 and 9. These show that the tensile strength and modulus at 100% elongation increased with increasing the weight ratio of D_4 to SBR, but the elongation at break decreased with increasing the weight ratio of D_4 to SBR, while all remained reasonably constant when the weight ratio of D_4 to SBR was higher than 0.20.

Compared with the SBR vulcanizates, the enhancement of the tensile strength and modulus at 100% elongation in the SBR-*g*-D_4 vulcanizates may be due to the higher crosslinking degree than in SBR, that is, the crosslinking degree of the SBR-*g*-D_4 vulcanizates can be mainly attributed to two contributions: sulfur crosslinkage and D_4 crosslinkage; these lead to the strengthening of the interface which could subsequently promote an easier stress transfer across the molecular chains.[49] At the same time, the higher crosslinking density of SBR-*g*-D_4 increases the rigidity of rubber molecular chains, resulting in a decrease in the elongation at break.

The effects of the D_4 content on the silica content, curing characteristics and mechanical properties of SBR-*g*-D_4 having been thoroughly investigated, it was found that the optimal weight ratio of D_4 to SBR is 0.20. The SBR-*g*-D_4 latex with the optimal weight ratio was then mixed with a certain amount of TEOS at 50 °C.

3.3 Sol–gel reaction of TEOS in the SBR-*g*-D_4 latex

3.3.1 *In situ* generated silica content in reinforced SBR-*g*-D_4 and utilization efficiency of TEOS. Fig. 10 shows the effect of the weight of TEOS (5.00–45.00 g) on the *in situ* generated silica (SiO_2) content in the reinforced SBR-*g*-D_4 at 50 °C, with the TEOS being added after the graft copolymerization.

The *in situ* generated silica content increased with increasing TEOS weight, although it remained constant after the weight of TEOS was more than 35 g. As the *in situ* silica was generated by the sol–gel reaction of TEOS, the silica content was thus controlled by the weight of TEOS and the *in situ* formed silica content increased with increasing TEOS weight. However, this sol–gel technique may be restricted by the amount of D_4 grafted SBR due to the polarity differences between SBR and silica.[50] For excessively TEOS filled composites (where the weight of TEOS was higher than 35 g), a constant *in situ* silica content was observed. This is due to the fact that, relative to the weight of TEOS, the weight of the SBR-*g*-D_4 is limited, and as a result, the extra *in situ* silica generated from TEOS agglomerates and separates out from the SBR-*g*-D_4 latex, resulting in the relatively constant *in situ* generated silica content. Similarly, with the limited amount of SBR-*g*-D_4 mixed with the TEOS, the utilization of TEOS decreased with the increasing weight of TEOS, and then became constant, which is also shown in Fig. 10.

3.3.2 Curing characteristics of the *in situ* generated silica reinforced SBR-*g*-D_4 vulcanizates. Table 3 shows the effect of *in situ* generated silica content on the curing time of reinforced SBR-*g*-D_4. This shows that the t_{s2} and t_{90} increased with increasing *in situ* generated silica (SiO_2) content, which is attributed to the absorption of the accelerator by the –OH groups on the *in situ* generated SiO_2 surface; this consequently lowered the accelerator activity and slowed down the sulfur vulcanizing reaction, resulting in the delayed curing time of the *in situ* generated silica reinforced SBR-*g*-D_4.[51]

With respect to the t_{90}–t_{10}, it increased with increasing weight of TEOS. It is possible that the *in situ* generated SiO_2 was grafted onto the SBR-*g*-D_4 chains by the chemical bond between –Si–O– groups in SBR-*g*-D_4 and SiO_2, which could increase the crosslinking degree of SBR-*g*-D_4, thereby resulting in the increase in t_{90}–t_{10}.

Fig. 11 shows the effect of the *in situ* generated SiO_2 content on the torque (ML and MH) of reinforced SBR-*g*-D_4 vulcanizates. The ML and MH are closely related to the interaction between SBR-*g*-D_4 and SiO_2. The ML and MH were found to be increased with increasing silica content, indicating a good interaction between SBR-*g*-D_4 and SiO_2. This is due to the improvement of the interaction between the SBR-*g*-D_4 and SiO_2 by the –Si–O–Si– groups in the molecular chains of the SBR-*g*-D_4.[52] For excessively silica filled composites (the content of silica was higher than 13.70%), constant ML and MH were observed, due to the fact that, relative to the *in situ* silica content, the –Si–O– groups in the SBR-*g*-D_4 are limited. As a result, an excess amount of *in situ* generated silica cannot be inserted into the networks of SBR-*g*-D_4 molecular chains to enhance the interaction between SBR-*g*-D_4 molecular chains and SiO_2, resulting in the relatively constant ML and MH when the silica content is higher than 13.70%.

3.3.3 Mechanical properties of the silica reinforced SBR-*g*-D_4 and *in situ* generated silica reinforced SBR-*g*-D_4 vulcanizates. The effects of the silica content on the stress–strain behavior of the silica reinforced SBR and *in situ* generated silica reinforced

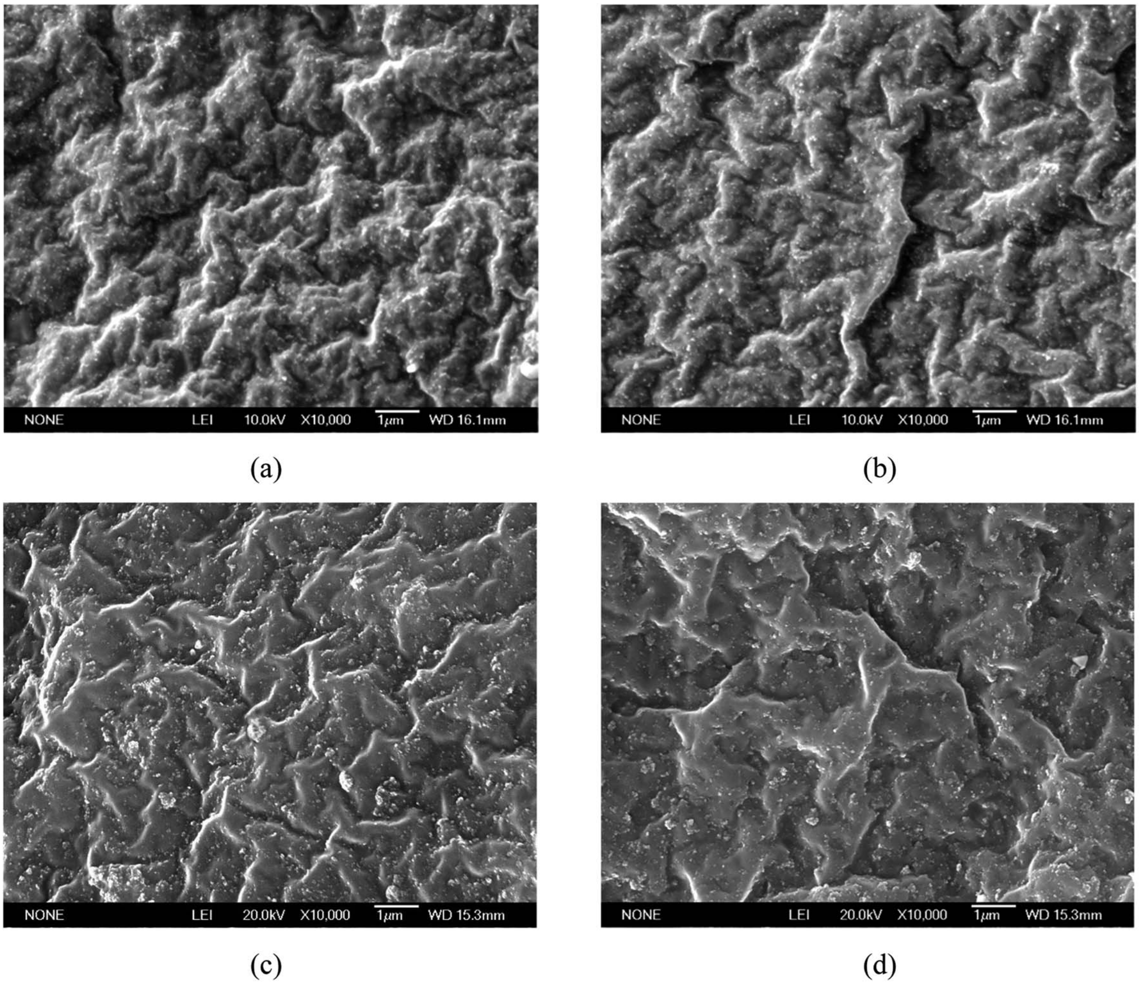

(a) (b) (c) (d)

Fig. 15 Morphological images of the tensile fracture surface of *in situ* generated silica reinforced SBR-*g*-D4 with a varying silica content: (a) 7.9%, (b) 9.32%, (c) 13.7%, and (d) 18.05%.

SBR-*g*-D_4 are presented in Fig. 12 and 13, respectively, and the detailed tensile strength and elongation at break data are summarized in Table 4.

Fig. 12 and 13 both show that the stress–strain properties of the reinforced SBR-*g*-D_4 composites gradually improve with an increase in the silica content in the composite. The improvement in the mechanical properties is attributed to the rubber filler interaction. At the same time, the stronger modulus in the *in situ* generated silica reinforced SBR-*g*-D_4 vulcanizates is due to more regularity and the presence of entanglements.

Table 4 shows that the tensile strength increased with increasing *in situ* generated SiO_2 content, and peaked at an SiO_2 content of 13.70%, becoming relatively constant at the higher SiO_2 content. This is due to the reinforcement effect of *in situ* generated silica particles on the SBR-*g*-D_4 matrix networks.[53] This result correlates well with the MH and ML data for the reinforced SBR-*g*-D_4 noted above, due to the limited –Si–O– functional groups in the SBR-*g*-D_4. The elongation at break of the reinforced SBR-*g*-D_4 vulcanizates decreased with the increasing *in situ* generated silica content. This is due to more silica-SBR-*g*-D_4 interactions and higher crosslink densities.[54] At the same time, the tensile strength of the *in situ* generated silica reinforced SBR-*g*-D_4 was higher than that of the silica reinforced SBR-*g*-D_4, which is attributed to the higher crosslinking degree in the SBR-*g*-D_4 matrix and the strong chemical bond between SBR-*g*-D_4 molecular chains and *in situ* generated silica.

All these results may also prove that SBR-*g*-D_4 can generate a chemical interaction with *in situ* generated SiO_2 in the silica-reinforced SBR-*g*-D_4, according to the mechanism proposed in Scheme 1.[55,56]

3.3.4 Dynamic mechanical analysis of the silica reinforced SBR-*g*-D_4 and *in situ* generated silica reinforced SBR-*g*-D_4 vulcanizates. It was reported that the loss tangent (tan δ) at 50–80 °C is an indication of tire rolling resistance, and the lower the value of tan δ at 50–80 °C, the better the rolling resistance of tires. In a laboratory scale test, the tan δ at -20 to 0 °C of the vulcanizates is an indication of wet skid resistance, and the higher the value of tan δ at -20 to 0 °C, the better the wet skid resistance of tires.[56,57]

The tan δ values of the silica reinforced SBR, SBR-*g*-D_4 and *in situ* generated silica reinforced SBR-*g*-D_4 vulcanizates are shown in Fig. 14. Compared with the tan δ value of silica reinforced SBR vulcanizates, the tan δ value at -20 to 0 °C of the silica reinforced SBR-*g*-D_4 vulcanizates was higher, indicating the better wet skid resistance of the silica reinforced SBR-*g*-D_4 vulcanizates. At the same time, the tan δ value at -20 to 0 °C of the *in situ* generated silica reinforced SBR-*g*-D_4 vulcanizates was highest of all, indicating an increased wet skid resistance, while the tan δ at 50–80 °C of the *in situ* generated silica reinforced SBR-*g*-D_4 vulcanizates was lower, implying a decrease in rolling resistance. This may be attributed to a strong interaction between SBR and *in situ* generated silica and the additional linkages created by D_4.

3.4. Morphology of the *in situ* generated silica reinforced SBR-*g*-D_4 vulcanizates

The morphological behavior of the tensile fracture surface (at 7.9%, 9.32%, 13.7%, and 18.05% *in situ* generated silica content) was analyzed by a scanning electron microscopy (SEM) study, as shown in Fig. 15(a), (b), (c), and (d) , respectively. The SEM images clearly indicate the good silica filler dispersion in all the reinforced SBR-*g*-D_4 vulcanizates. This is due to the fact that SBR-*g*-D_4 may act as a compatibilizer between ungrafted SBR and the *in situ* generated silica particles, which increases the dispersion of the silica particles to a greater extent. However, compared with the fracture surfaces seen in Fig. 15(c) and (d), the *in situ* generated silica reinforced SBR-*g*-D_4 vulcanizates (Fig. 15(a) and (b)) exhibit a rugged surface when the silica content is lower than 9.32%. This is because of the higher crosslinking degree in the SBR-*g*-D_4 matrix and the strong chemical bond between SBR-*g*-D_4 molecular chains and *in situ* generated silica, which improves the plasticity of *in situ* generated silica reinforced SBR.[58]

4. Conclusions

A new *in situ* generated silica reinforced SBR-*g*-D_4 vulcanizate has been developed from SBR latex through the grafting and sol–gel reaction of TEOS. The chemical structures of SBR-*g*-D_4 and *in situ* generated silica reinforced SBR-*g*-D_4 were assessed by FTIR, Raman and XPS analysis. After grafting, the constant silicon content and GER were 1.72% and 0.13 wt% when the weight ratio of D_4 to SBR was 0.20; under this condition, the tensile strength of SBR-*g*-D_4 vulcanizates could reach 4.84 MPa. The SBR-*g*-D_4 was then reinforced by the *in situ* generated silica formed by the sol–gel reaction of TEOS in latex; the constant *in situ* generated silica content was 18.05%, and the tensile strength of the *in situ* generated silica reinforced SBR-*g*-D_4 was found to have been significantly enhanced. The tensile strength of the *in situ* generated silica reinforced SBR-*g*-D_4 vulcanizates was increased significantly compared to that of pristine rubber vulcanizates, due to the formation of chemical bonds between –Si–O– groups in SBR-*g*-D_4 and *in situ* generated silica. SEM images clearly indicate the good silica filler dispersion of all of the reinforced SBR-*g*-D_4 vulcanizate matrices.

Conflicts of interest

There are no conflicts to declare.

Acknowledgements

The authors are grateful for support and funding from the National Natural Science Foundation of China (No. 51603168), and the Natural Science Foundation of Shaanxi Province (No. 2017JQ2011).

References

1 A. Tunlert, P. Prasassarakich and S. Poompradub, Effect of Modified Silica Particles with Phenyltriethoxysilane on Mechanical and Thermal Properties of Natural Rubber Composites, *Macromol. Symp.*, 2015, **354**, 62–68.
2 Y. Li, B. Han, L. Liu, F. Zhang and S. Wen, Surface modification of silica by two-step method and properties of

solution styrene butadiene rubber (SSBR) nanocomposites filled with modified silica, *Compos. Sci. Technol.*, 2013, **88**, 69–75.

3 K. Stockelhuber, A. Svistkov, A. Pelevin and G. Heinrich, Impact of filler surface modification on large scale mechanics of styrene butadiene/silica rubber composites, *Macromolecules*, 2011, **44**(11), 4366–4381.

4 C. Lan, S. ha, K. Tridib and T. Lei, Synergistic reinforcement of silanized silica-graphene oxide hybrid in natural rubber for tire-tread fabrication: a latex based facile approach, *Composites, Part B*, 2019, **161**, 667–676.

5 C. Sun, S. Wen and H. Ma, Improvement of Silica Dispersion in Solution Polymerized Styrene-Butadiene Rubber *via* Introducing Amino Functional Groups, *Ind. Eng. Chem. Res.*, 2019, **58**, 1454–1461.

6 S. Prasertsri and N. Rattanasom, Mechanical and damping properties of silica/natural rubber composites prepared from latex system, *Polym. Test.*, 2011, **30**, 515–526.

7 K. Sengloyluan, K. Sahakaro, W. K. Dierkes and J. W. M. Noordermeer, Silane grafted natural rubber and its compatibilization effect on silica-reinforced rubber tire compounds, *eXPRESS Polym. Lett.*, 2017, **11**, 1003–1022.

8 B. C. Zhong, Z. X. Jia, D. C. Hu, Y. F. Luo, D. M. Jia and F. Liu, Enhancing interfacial interaction and mechanical properties of styrene-butadiene rubber composites *via* silica-supported vulcanization accelerator, *Composites, Part A*, 2017, **96**, 129–136.

9 S. Pongsathit and C. Pattamaprom, Irradiation grafting of natural rubber latex with maleic anhydride and its compatibilization of poly(lactic acid)/natural rubber blends, *Radiat. Phys. Chem.*, 2018, **144**, 13–20.

10 B. Tian, W. Dong and Y. G. Liu, Grafting poly(vinyl alcohol) onto polybutadiene rubber latex particles by pre-irradiation, *Radiat. Phys. Chem.*, 2017, **135**, 81–87.

11 N. H. Yusof, K. Kosugi, T. K. Song and S. Kawahara, Preparation and characterization of poly(stearyl methacrylate) grafted natural rubber in latex stage, *Polymer*, 2016, **88**, 43–51.

12 P. Saramolee, N. Lopattananon and K. Sahakaro, Preparation and some properties of modified natural rubber bearing grafted poly(methyl methacrylate) and epoxide groups, *Eur. Polym. J.*, 2014, **56**, 1–10.

13 P. Juntuek, C. Ruksakulpiwat, P. Chumsamrong and Y. Ruksakulpiwat, Glycidyl methacrylate grafted natural rubber: synthesis, characterization, and mechanical property, *J. Appl. Polym. Sci.*, 2011, **122**, 3152–3159.

14 N. T. Ha, K. Kaneda, Y. Naitoh, L. Fukuhara, K. Kosugi and S. Kawahara, Preparation and graft-copolymerization of hydrogenated natural rubber in latex stage, *J. Appl. Polym. Sci.*, 2015, **132**, 42435–42442.

15 N. Pukkate, T. Kitai, Y. Yamamoto, T. Kawazura and S. Kawahara, Nano-matrix structure formed by graft-copolymerization of styrene onto natural rubber, *Eur. Polym. J.*, 2007, **43**, 3208–3214.

16 C. J. Yin and Q. Y. Zhang, Studies on preparation and properties of vinyltriethoxysilane-grafted styrene-butadiene rubber, *J. Appl. Polym. Sci.*, 2011, **119**, 2808–2814.

17 M. Takamura, T. Yamauchi and N. Tsubokawa, Grafting and crosslinking reaction of carboxyl-terminated liquid rubber with silica nanoparticles and carbon black in the presence of Sc(OTf)$_3$, *React. Funct. Polym.*, 2008, **68**, 1113–1118.

18 W. Chueangchayaphan, N. Chueangchayaphan and S. M. VTanrattanakul, Influences of the grafting percentage of natural rubber-graft-poly(2-hydroxyethyl acrylate) on properties of its vulcanizates, *Polym. Int.*, 2018, **67**, 739–746.

19 N. H. Yusof, K. Kosugi, T. K. Song and S. Kawahara, Preparation and characterization of poly(stearyl methacrylate) grafted natural rubber in latex stage, *Polymer*, 2016, **88**, 43–51.

20 C. Zhang, C. Man, Y. Pan, W. Wang, L. Jiang and Y. Dan, Toughening of polylactide with natural rubber grafted with poly(butyl acrylate), *Polym. Int.*, 2011, **60**, 1548–1555.

21 J. Peng, M. L. Wang, J. L. Qiao and G. S. Wei, Radiation-induced grafting polymerization of MMA onto polybutadiene rubber latex, *Radiat. Phys. Chem.*, 2005, **72**, 739–743.

22 N. C. Dafader, M. E. Haque, F. Akhtar and M. U. Ahmad, Study on grafting of different types of acrylic monomers onto natural rubber by γ-rays, *Radiat. Phys. Chem.*, 2006, **75**, 168–172.

23 C. C. Ferraz, G. H. Varca, J. C. Ruiz, P. S. Lopes and E. Bucio, Radiation-grafting of thermo- and pH-responsive poly(N-vinylcaprolactam-co-acrylic acid) onto silicone rubber and polypropylene films for biomedical purposes, *Radiat. Phys. Chem.*, 2014, **97**, 298–303.

24 T. Ohashi, A. Tohsan and Y. Ikeda, Role of *in situ* generated silica for rubber science and technology, *Polym. Int.*, 2017, **66**, 250–259.

25 B. P. Kapgate, C. Y. Das, A. Das, D. Basu, S. Wiessner, U. Reuter and G. Heinrich, Reinforced chloroprene rubber by *in situ* generated silica particles: Evidence of bound rubber on the silica surface, *J. Appl. Polym. Sci.*, 2016, **133**(30), 43717–43726.

26 Q. Y. Li, X. Li, D. Lee, Y. Fan, B. U. Nam, J. E. Lee and U. R. Cho, Hybrid of bamboo charcoal and silica by tetraethoxysilane hydrolysis over acid catalyst reinforced styrene-butadiene rubber, *J. Appl. Polym. Sci.*, 2018, **135**, 46219–46225.

27 T. Atitaya, K. Ryota and Y. Ikeda, A model filler network in nanocomposites prepared by *in situ* silica filling and peroxide cross-linking in natural rubber latex, *Colloid Polym. Sci.*, 2015, **293**, 2083–2093.

28 F. Bignotti, S. Borsacchi, R. de Santis, M. Geppi, M. Messori and U. P. Sudhakaran, Interrelation between preparation conditions, structure, and mechanical reinforcement in isoprene rubber filled with *in situ* generated silica, *J. Appl. Polym. Sci.*, 2012, **125**, 1398–1412.

29 N. Sakdinun, Y. Satit, C. Supphathee, Y. Toshiyuki and N. T Takashi, Chawalit. Mesostructured natural rubber/*in situ* formed silica nanocomposites: a simple way to prepare mesoporous silica with hydrophobic properties, *Microporous Mesoporous Mater.*, 2018, **259**, 79–88.

30 V. Raman, A. D. Sankar and K. W. Stoeckelhuber, Improvement of mechanical performance of solution

styrene butadiene rubber by controlling the concentration and the size of *in situ* derived sol-gel silica particles, *RSC Adv.*, 2016, **6**, 33643–33655.

31 T. Sittiphan, P. Prasassarakich and S. Poompradub, Styrene grafted natural rubber reinforced by *in situ* silica generated *via* sol-gel technique, *Mater. Sci. Eng., B*, 2014, **181**, 39–45.

32 N. Watcharakul, S. Poompradub and P. Prasassarakich, *In situ* silica reinforcement of methyl methacrylate grafted natural rubber by sol–gel process, *J. Sol-Gel Sci. Technol.*, 2011, **58**, 407–418.

33 C. Yin and Q. Zhang, *In situ* silica reinforcement of vinyltriethoxysilane-grafted styrene butadiene rubber by sol-gel process, *J. Appl. Polym. Sci.*, 2013, **128**, 2262–2268.

34 C. Yin, Q. Zhang and J. Liu, Preparation, properties of *in situ* silica modified styrene butadiene rubber and its silica-filled composites, *Polym. Compos.*, 2018, **39**, 22–28.

35 J. Liang, L. He, W. Li and H. Luo, Synthesis and analysis of properties of a new core–shell silicon-containing fluoroacrylate latex, *Polym. Int.*, 2009, **58**, 1283–1290.

36 S. Jiang and X. L. TQiu, Kinetic study on the ring-opening polymerization of octamethylcyclotetrasiloxane (D_4) in miniemulsion, *Polymer*, 2010, **51**, 4087–4094.

37 C. Lia, Y. Wang, Z. Yuan and L. Ye, Construction of sacrificial bonds and hybrid networks in EPDM rubber towards mechanical performance enhancement, *Appl. Surf. Sci.*, 2019, **484**, 616–627.

38 K. Huang, Y. Liu and D. Wu, Synthesis and characterization of polyacrylate modified by polysiloxane latexes and films, *Prog. Org. Coat.*, 2014, **77**, 1774–1779.

39 W. Kangwansupamonko, R. G. Gilbert and S. Kiatkamjornwong, Modification of natural rubber by grafting with hydrophilic vinyl monomers, *Macromol. Chem. Phys.*, 2005, **206**, 2450–2460.

40 R. Scotti, L. Wahba, M. Crippa, M. Arienzo and R. Donetti, Rubber-silica nanocomposites obtained by *in situ* sol–gel method: particle shape influence on the filler-filler and filler-rubber interactions, *Soft Matter*, 2012, **8**, 2131–2143.

41 N. J. Trujillo, Q. G. Wu and K. K. Gleason, Ultralow Dielectric Constant Tetravinyltetramethylcyclotetrasiloxane Films Deposited by Initiated Chemical Vapor Deposition (iCVD), *Adv. Funct. Mater.*, 2010, **20**, 607–616.

42 P. L. Lamaa, C. Ferronato, S. Prakash and L. Fine, Photocatalytic oxidation of octamethylcyclotetrasiloxane (D_4): towards a better understanding of the impact of volatile methyl siloxanes on photocatalytic systems, *Appl. Catal., B*, 2014, **156–157**, 438–446.

43 K. Huang, Y. L. Liu and D. F. Wu, Synthesis and characterization of polyacrylate modified by polysiloxane latexes and films, *Prog. Org. Coat.*, 2014, **77**, 1774–1779.

44 P. Satraphan, A. Intasiri, V. Tangpasuthadol and S. Kiatkamjornwong, Effects of methyl methacrylate grafting and *in situ* silica particle formation on the morphology and mechanical properties of natural rubber composite films, *Polym. Adv. Technol.*, 2009, **20**, 473–486.

45 T. Kochthongrasamee, P. Prasassarakich and S. Kiatkamjornwong, Effects of redox initiator on graft copolymerization of methyl methacrylate onto natural rubber, *J. Appl. Polym. Sci.*, 2006, **101**, 2587–2601.

46 A. Tunlert, P. Prasassarakich and S. Poompradub, Effect of Modified Silica Particles with Phenyltriethoxysilane on Mechanical and Thermal Properties of Natural Rubber Composites, *Macromol. Symp.*, 2015, **354**, 62–68.

47 H. Yangthong, S. Pichaiyut, S. Jumrat, S. Wisunthorn and C. Nakason, Mechanical, thermal, morphological, and curing properties of geopolymer filled natural rubber composites, *J. Appl. Polym. Sci.*, 2019, **136**, 47346–47363.

48 C. J. Yin, Q. Y. Zhang and J. W. Gu, Cure characteristics and mechanical properties of styrene-butadiene rubber/hydrogenatedacrylonitrile-butadiene rubber/silica composites, *J. Polym. Res.*, 2011, **18**, 2487–2494.

49 J. Jayadevan, R. Alexb and U. Gopalakrishnapanicker, Deproteinised natural rubber latex grafted poly(dimethylaminoethylmethacrylate)-poly(vinyl alcohol) blend membranes: synthesis, properties and application, *Int. J. Biol. Macromol.*, 2018, **107**, 1821–1834.

50 A. M. Shanmugharaj and H. Ryu, Influence of aminosilane functionalized carbon nantubes on the rheometric, mechanical, electrical and thermal degradation properties of epoxidized natural rubber nanocomposites, *Polym. Int.*, 2013, **62**, 1433–1441.

51 Y. Z. Song, J. H. Yu, D. Dai, L. X. Song and N. Jiang, Effect of silica particles modified by in situ and ex situ methods on the reinforcement of silicone rubber, *Mater. Des.*, 2014, **64**, 687–693.

52 C. J. Yin and Q. Y. Zhang, Free-radical emulsion copolymerization of styrene with butadiene and vinyl triethoxysilane with a cumene hydroperoxide redox initiator, *J. Appl. Polym. Sci.*, 2019, **136**, 47896–47902.

53 L. N. Carli, C. R. Roncato, A. Zanchet, R. S. Mauler, M. Giovanela, R. N. Brandalise and J. S. Crespo, Characterization of natural rubber nanocomposites filled with organoclay as a substitute for silica obtained by the conventional two-roll mill method, *Appl. Clay Sci.*, 2011, **52**, 56–61.

54 K. Sengloyluan, K. Sahakaro, W. K. Dierkes and J. W. M. Noordermeer, Silane grafted natural rubber and its compatibilization effect on silica-reinforced rubber tire compounds, *eXPRESS Polym. Lett.*, 2017, **11**, 1003–1022.

55 H. D. Luginsland, J. Frohlich and A. Wehmeier, Influence of different silanes on the reinforcement of silica-filled rubber compounds, *Rubber Chem. Technol.*, 2002, **75**, 563–579.

56 K. Sengloyluan, K. Sahakaro, W. K. Dierkes and J. W. M. Noordermeer, Silica-reinforced tire tread compounds compatibilized by using epoxidized natural rubber, *Eur. Polym. J.*, 2014, **51**, 69–79.

57 G. Arun and S. De, Dependence of Physical Properties and Processing Behavior of Blends of Silicone Rubber and Fluororubber on Blend Morphology, *Rubber Chem. Technol.*, 2004, **77**, 856–872.

58 S. Mohapatra, R. Alex and G. B. Nando, Cardanol grafted natural rubber: A green substitute to natural rubber for enhancing silica filler dispersion, *J. Appl. Polym. Sci.*, 2016, **133**, 43057–43062.